RSC Advances

PAPER

View Article Online
View Journal | View Issue

Cite this: *RSC Adv.*, 2021, **11**, 7454

Photolysis of the BODIPY dye activated by pillar[5]arene†

Haifan Zhang,[a] Long Wang,[a] Puyang Dong,[a] Shuqiang Mao,[a] Pu Mao*[a] and Guoxing Liu*[ab]

Received 9th October 2020
Accepted 22nd January 2021

DOI: 10.1039/d0ra08611h

rsc.li/rsc-advances

Here, a pseudo[3]rotaxane comprising a fluorescent BODIPY derivative and pillar[5]arene was conveniently fabricated *via* host–guest complexation. Importantly, in this system, the efficient photodecomposition of the BODIPY derivative in the presence of pillar[5]arene was witnessed upon irradiation at 311 nm light, which was demonstrated *via* UV-Vis absorption, fluorescence emission, NMR and HR-MS spectroscopy techniques, but the only BODIPY dye in the absence of pillar[5]arene couldn't undergo photodegradation. We demonstrated that pillar[5]arene could act as an activator to trigger the photodegradation reaction of BODIPY derivatives *via* free radical reactions even without supramolecular interactions. The present results provide a new strategy for the efficient photolysis of organic dyes.

Superfluous organic dyes are one of the most serious contamination sources that are discharged at will, which is a cause for concern. The efficient elimination of organic dyes is a hugely challenging problem that needs and remains to be solved. Most approaches, such as membrane separation,[1] activated carbon adsorption,[2] ion exchange on synthetic adsorbent resins[3] and coagulation by chemical agents,[4] were adopted to dispose of the organic dye pollution. However, these superfluous organic dyes cannot be thoroughly degraded *via* these conventional methods. Light is considered one of the most desirable stimuli because of its non-invasiveness, easy controllability, low cost, and ubiquity.[5] Owing to the above-mentioned advantages, light is often utilized as an effective strategy to manage responsive materials, which have been applied in numerous research fields, such as separation technology,[6] photolithography,[7] photocontrolled singlet oxygen generation,[8] optical memory storage,[9] and photomodulated control-release of anions.[10] Among numerous stimuli-responsive systems, photolyzable matrices that can irreversibly decompose after irradiation have aroused wide research interests in the design and construction of photodegradable materials, controlled drug release systems and tissue engineering systems.[11] The supramolecular method was alternatively used to develop photodegradable materials.[12] Recently, Liu *et al.* developed a photoresponsive amphiphilic supramolecular assembly that achieved efficient photolysis of anthracene derivatives *via* calixarene-induced aggregation.[13] Subsequently, they employed several multi-charged macrocycles such as water-soluble cyclodextrins, calixarenes, crown ethers and cucurbiturils as platforms for the rapid and broad spectral photodecomposition of aromatic dyes.[14] Although there are a few reports on the construction of photodegradable supramolecular assemblies, the fabrication of photoresponsive supramolecular systems equipped with photolysis remains highly unexplored. Consequently, it is still necessary to develop novel high-efficiency photolyzable supramolecular materials. Pillararenes (particularly pillar[5]arene and pillar[6]arene), as a new type of supramolecular macrocycles, have been used as a host to construct photodegradable materials.[15] For instance, Wang *et al.* prepared a bola-type supra-amphiphilic photoresponsive supramolecular material based on water-soluble pillar[5]arene, achieving the photodecomposition of the 9,10-dialkoxyanthracene group.[16]

Due to excellent photophysical and photochemical properties such as good photostability and fluorescence quantum yield,[17] BODIPY dyes have been generally applied in bioimaging and fluorescent sensing,[18] photodynamic therapy,[19] advanced optical materials,[20] *etc*. However, the elimination of surplus and used BODIPY dyes and other fluorescent dyes has gradually become a major issue to be addressed due to use and waste of large amounts of organic dyes applied in living matter. Furthermore, some BODIPY derivatives have high cytotoxicity.[21] Consequently, it is crucial to seek a simple and effective method for dealing with excess and useless organic pollutants. Herein, to the best of our knowledge, we first put forward a new way for the efficient photolysis of BODIPY dyes *via* free radical reaction triggered by **P5**.

The BODIPY dye **G-BODIPY** and pillar[5]arene (**P5**) acted as the guest and host, respectively. Their synthetic routes were prepared by simple steps, as shown in Scheme 1. 3,4-Dihydroxybenzaldehyde (**1**) reacted with propargyl bromide to

[a]*College of Chemistry and Chemical Engineering, Henan University of Technology, Zhengzhou 450001, P. R. China. E-mail: gxliu@henau.edu.cn; maopu@haut.edu.cn*

[b]*College of Science, Henan Agricultural University, Zhengzhou, 450002, China*

† Electronic supplementary information (ESI) available: Synthesis and characteristics of new compounds and other data. See DOI: 10.1039/d0ra08611h

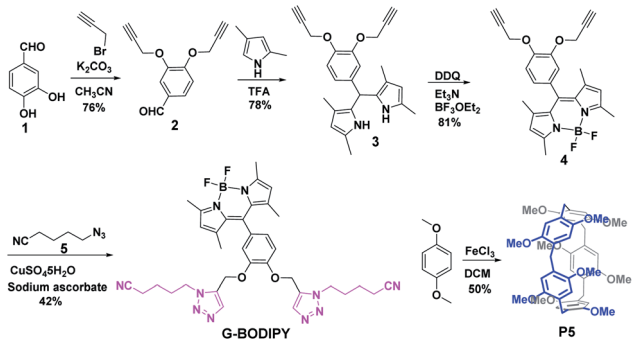

Scheme 1 The synthesis route of **G-BODIPY** and **P5**.

obtain compound (**2**). Subsequently, the reaction of (**2**) and pyrrole catalyzed by TFA produced substance (**3**). Then, (**3**) encountered with DDQ, Et_3N and $BF_3 \cdot OEt_2$ in succession to give compound (**4**). Finally, the click reaction of (**4**) and (**5**) by the catalyzation of $CuSO_4 \cdot 5H_2O$ and sodium ascorbate prepared **G-BODIPY**. Macrocyclic host **P5** was synthesized by 1,4-dimethoxybenzene by the catalyzation of $FeCl_3$.

It is well-known that a strong binding ability ($K_a = 1.2 \times 10^4$ M^{-1}) exists between **P5** and the neutral guests bearing two or three short alkyl chains with a triazole site and a cyano site at either end in chloroform.[22] Therefore, we speculated that **G-BODIPY** would assemble with **P5** by an equivalent proportion of 1 : 2 (guest/host) and strong complexation. As displayed in Fig. S5,† an NMR titration experiment was performed. From the NMR titration spectroscopy, an apparent upfield shift of the resonance for methylene in the guest (H_{a-d}) was observed, and their integral areas remained unchanged with the continuous addition of 2 equiv. **P5**, indicating the 2 : 1 host–guest binding stoichiometry. The complex stability constant (K_S) was determined as 5.66×10^6 M^{-2} using the ^{1}H NMR single point method (see Fig. S5 and computational method in ESI†). Clearly, the assembled model of **G-BODIPY** and **P5** are manifested in Scheme 2. The corresponding proof was provided by the ^{1}H NMR spectroscopic contrast, indicating the apparent upfield shift for the resonance of methylene (H_{a-d}) of the guest, which implies the occurrence of an assembling behavior and the formation of a new supramolecular assembly **G-BODIPY⊂P5$_2$** (Fig. 1). Furthermore, as shown in Fig. S6 and S7,† the absorbance (at 504 nm) and fluorescence intensity (at 517 nm) of **G-BODIPY** increased slightly with the addition of **P5**,

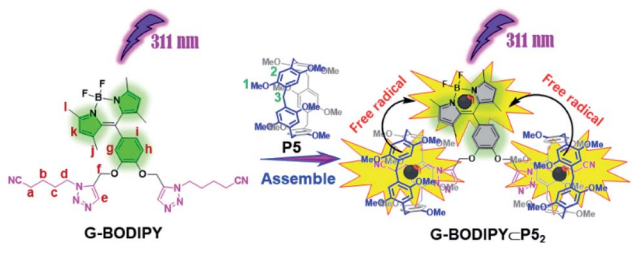

Scheme 2 Schematic illustration of formation pattern of assembly **G-BODIPY⊂P5$_2$** and photolysis of the BODIPY guest induced by **P5**.

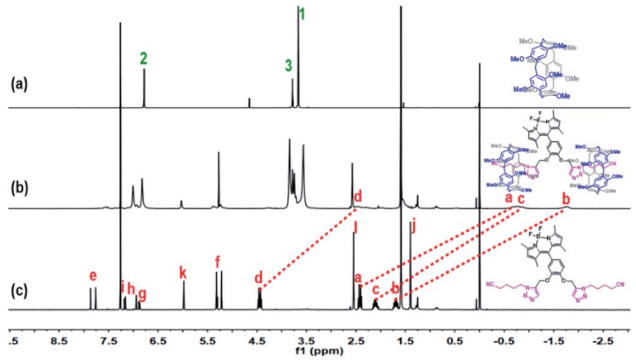

Fig. 1 ^{1}H NMR (400 MHz, $CDCl_3$) spectra of (a) **P5**, (b) assembly **G-BODIPY⊂P5$_2$** and (c) guest **G-BODIPY**. [**P5**] = 2[**G-BODIPY**] = 6×10^{-3} mol L^{-1}.

implying the formation of the host-guest complex **G-BODIPY⊂P5$_2$**. Therefore, **G-BODIPY** and **P5** self-assembled to a [3]pseudorotaxane **G-BODIPY⊂P5$_2$** in chloroform (Scheme 2).

To our surprise, as illustrated in Fig. 2a, when the sample containing **G-BODIPY⊂P5$_2$** was irradiated using 311 nm light, the absorbance at 295 nm and 503 nm (assigned to BODIPY unit) significantly declined by 83% (503 nm) with four isosbestic points at 286 nm, 308 nm, 458 nm and 518 nm, respectively, implying that the BODIPY unit of **G-BODIPY** was dramatically destroyed. The photochemical quantum yield (311 nm light irradiation) of the pseudo[3]rotaxane was determined to be 0.34, and the test method was added in the ESI.† However, in the control experiment, only the guest **G-BODIPY** expressed no obvious change under the same condition,

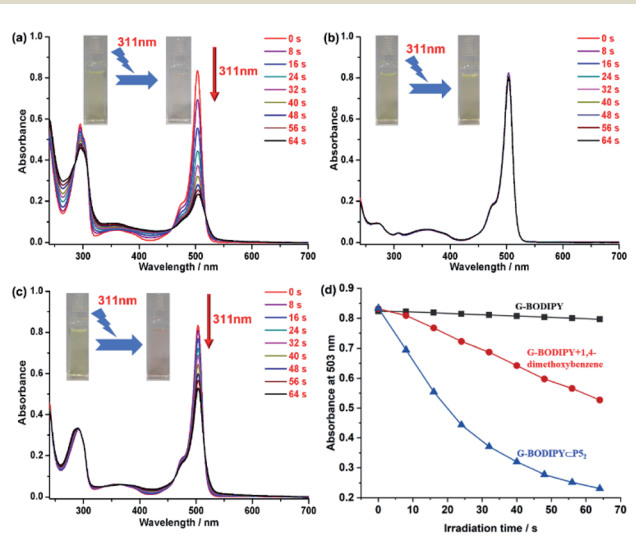

Fig. 2 (a) The variation of UV-Vis absorption spectra of **G-BODIPY** with **P5** upon continuous irradiation of 311 nm. (b) The variation of the UV-Vis absorption spectra of **G-BODIPY** upon continuous irradiation of 311 nm. (c) The variation of UV-Vis absorption spectra of **G-BODIPY** with 10 eq. **PDME** upon continuous irradiation of 311 nm. (d) The variation of absorbance of **G-BODIPY**, **G-BODIPY** with 10 eq. **PDME** and **G-BODIPY** with **P5** at 503 nm upon continuous irradiation of 311 nm. [**G-BODIPY**] = 1.0×10^{-5} mol L^{-1}.

indicating that its structure exhibited invariability upon irradiation at 311 nm. Furthermore, we selected *p*-phenyl dimethyl ether (**PDME**), which is 5 equivalents to the host (**P5**), to evaluate photodegradation performance. As shown in Fig. 2c, the absorbance of **G-BODIPY**/**PDME** at 503 nm decreased by only 43%, suggesting that **PDME** also influenced the photodegradation of the guest to some extent but unsatisfactory. More visually, the variation curve of the absorbance at 503 nm belonged to the BODIPY skeleton over irradiation time at 311 nm light for only **G-BODIPY**, **G-BODIPY**$\subset$**P5**$_2$ and **G-BODIPY**/**PDME**, as presented in Fig. 2d. Moreover, the color change of the samples containing **G-BODIPY**, **G-BODIPY**$\subset$**P5**$_2$ and **G-BODIPY**/**PDME** in the above irradiation process is visually shown in Fig. 2b, a and 2c (inset), which reveal that the sample containing **G-BODIPY**$\subset$**P5**$_2$ turned from yellow to almost colorless, while the others did not display a wide variation. The aforementioned investigation clearly illustrated that the intervention of **P5** caused the best photolysis efficiency of **G-BODIPY**.

In addition, we employed a fluorescence spectrometer to confirm if **P5** played a vital role in the photolysis of **G-BODIPY**. As expected, the fluorescence of **G-BODIPY**$\subset$**P5**$_2$ at 516 nm was quenched by 77%, which was consistent with the absorbance change (Fig. 3a). Intuitively, strong green fluorescence turned out to be very weak and nearly invisible to our eyes in the irradiation process (Fig. 3a, inset). On the contrary, no apparent variation of only **G-BODIPY** was observed in the fluorescence spectrum upon irradiation at 311 nm (Fig. 3b). Meanwhile, no fluorescent color and intensity changes were observed from photographs before and after irradiation (Fig. 3b, inset). Moreover, with regards to **BODIPY**/**PDME**, approximately 51% of fluorescence intensity was decreased, and its photodegradation efficiency was inferior to that of **G-BODIPY**$\subset$**P5**$_2$ (Fig. 3c). More visually, **G-BODIPY**$\subset$**P5**$_2$ manifested the highest fluorescence quenching efficiency (Fig. 3d), suggesting that **P5** induced high-efficiency photolysis of the BODIPY dye.

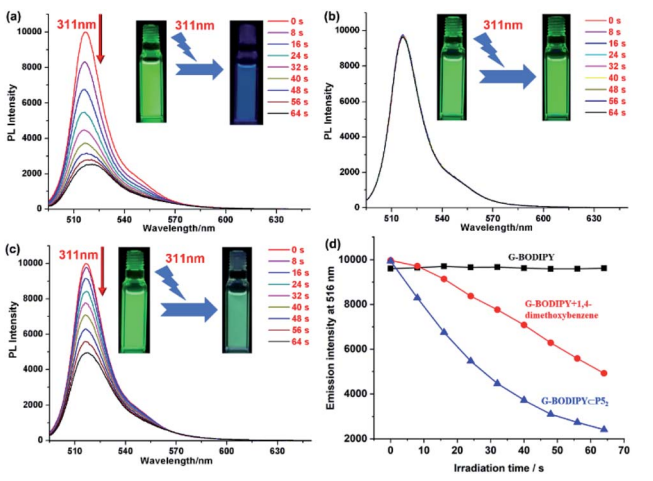

Fig. 3 (a) The variation of the fluorescence spectra of G-BODIPY with P5 upon continuous irradiation of 311 nm. (b) The variation of the fluorescence spectra of G-BODIPY upon continuous irradiation of 311 nm. (c) The variation of the fluorescence spectra of G-BODIPY with 10 eq. PDME upon continuous irradiation of 311 nm. (d) The variation of the fluorescence intensity of G-BODIPY, G-BODIPY with 10 eq. PDME and G-BODIPY with P5 at 516 nm upon continuous irradiation of 311 nm. [G-BODIPY] = 1.0×10^{-5} mol L^{-1}; excitation at 480 nm; slit = 1, 2.5.

Subsequently, to further verify the aforementioned consequence, we performed an NMR irradiation experiment for the sample containing **G-BODIPY**$\subset$**P5**$_2$ in $CDCl_3$. As shown in Fig. S8,† the resonance of the protons on the BODIPY group (H_k) in the assembly gradually disappeared with irradiation at 311 nm light for 3 h, indicating that the BODIPY group in **G-BODIPY**$\subset$**P5**$_2$ was almost completely damaged. In addition, we measured the HR-MS spectra of **P5** and **G-BODIPY**$\subset$**P5**$_2$ before and after the irradiation of 311 nm. As shown in Fig. S9–S12,† the HR-MS spectra of **P5** and **G-BODIPY**$\subset$**P5**$_2$ after irradiation showed the peaks at 768.3761 (assigned to **P5** + NH_4^+) and 681.3404 (belonged to **G-BODIPY**) both thoroughly disappeared and only some small molecular weight peaks were observed, revealing that **P5** and **G-BODIPY**$\subset$**P5**$_2$ were both broken into pieces. In contrast, when the sample containing only **G-BODIPY** was irradiated by 311 nm light, the resonance of the protons on the BODIPY group in the guest did not manifest any change (Fig. S13†). In addition, we conducted photoirradiation experiments of **P5** and **PDME** *via* UV-Vis absorption spectra upon irradiation at 311 nm, showing that photodecomposition reactions of **P5** and **PDME** occurred (Fig. S14 and S15†).

From the aforementioned investigation, the photolysis of **G-BODIPY** was efficiently activated by **P5**. We presumed that the three investigated manners of degradation were as follow: (a) energy transfer (as shown in Fig. S16,† **P5** and **PDME** with a specific absorbance at 311 nm can absorb 311 nm UV light into the solution containing **G-BODIPY** and deliver the absorbed light energy to **G-BODIPY**), (b) reactive oxygen species (photoreaction of **P5** and **PDME** caused by reactive oxygen species further triggered the photodecomposition of **G-BODIPY**), and (c) free radical species (photoreaction of **P5** and **PDME** caused by the free radical-activated photolysis of **G-BODIPY**). To clarify the credible manner, we subsequently performed a series of control experiments. As displayed in Fig. S17†, we directly employed a 500 nm wavelength light (which could also generate heat) on free **G-BODIPY** and complex **G-BODIPY**$\subset$**P5**$_2$ through the variation of UV-Vis absorption and emission spectra, and no changes were observed. The results implied that the degradation reaction was not caused by heat. Furthermore, the spectral overlap of UV-Vis absorption of **G-BODIPY** and fluorescence emission of **P5** (Fig. S18†) were performed and displayed almost very little degree of overlap (Fig. S19†). Thus, we could rule out the photolysis of the BODIPY dye caused by energy transfer from **P5** to **G-BODIPY**. Subsequently, we also investigated the photoirradiation experiments of **P5** and **G-BODIPY**$\subset$**P5**$_2$ under both aerobic and anaerobic conditions. The manifested results in the photoreactions mentioned above were not photooxidation reactions caused by oxygen (Fig. S20 and S21†). Then, we speculated that the photoreaction of **P5** caused by free radicals upon irradiation at 311 nm light could further trigger the photodecomposition reaction of **G-BODIPY**. To verify our speculation, we selected TEMPO as a free radical scavenger to

perform some control experiments. As displayed in Fig. S22b,† the absorption spectrum of **G-BODIPY⊂P5$_2$** in the presence of TEMPO showed no apparent change in comparison to that of **G-BODIPY⊂P5$_2$** in the absence of TEMPO (Fig. S22a†) upon irradiation at 311 nm light. Furthermore, a striking contrast for the absorbance variation of the pseudo[3]rotaxane at 503 nm in the presence and absence of TEMPO is presented in Fig. S22c.† Therefore, the above investigations demonstrated that photoreaction of **P5** caused by free radicals further triggered photodecomposition of **G-BODIPY** upon irradiation at 311 nm light. In the control experiments, we selected compound (**4**) that lacked the valeronitrile binding site to investigate its photoirradiation experiments in the presence and absence of **P5** using UV-Vis absorption and fluorescence emission spectra. As shown in Fig. S23 and S24,† the photolysis of compound (**4**) in the presence of **P5** without the host–guest complexation was also achieved upon irradiation at 311 nm light, which further implied that these photodecomposition reactions were caused by free radicals and not related to supramolecular interactions.

Conclusion

In summary, we synthesized a valeronitrile-modified BODIPY derivative *via* the "Click" reaction as a guest. Holosymmetric methoxyl-pillar[5]arene, as the host was prepared, and assembled with the BODIPY guest to form a pseudo[3]rotaxane. Importantly, pillar[5]arene as an activator could activate the high-efficiency photolysis of the BODIPY dye *via* free radical reactions, and was verified *via* UV-Vis absorption, fluorescence emission, NMR and HR-MS spectroscopy techniques. Through a series of control experiments, we also demonstrated that the photodecomposition reactions caused by free radicals were not related to supramolecular interactions. The study provides a new strategy to induce the efficient photodegradation of residual and useless organic dyes.

Conflicts of interest

There are no conflicts of interest to declare.

Acknowledgements

We thank the National Natural Science Foundation of China (No. 21801063), the Science and Technology Foundation of Henan Province (No. 192102210039), the Colleges and Universities Key Research Program Foundation of Henan Province (No. 19A150022) and China Postdoctoral Science Foundation (No. 2018M642767) for their financial support.

References

1 (*a*) S. P. Dharupaneedi, S. K. Nataraj, M. Nadagouda, K. R. Reddy, S. S. Shukla and T. M. Aminabhavi, *Sep. Purif. Technol.*, 2019, **210**, 850–866; (*b*) P. S. Goh and A. F. Ismail, *Desalination*, 2018, **434**, 60–80.

2 (*a*) N. Kannan and M. M. Sundaram, *Dyes Pigm.*, 2001, **51**, 25–40; (*b*) P. K. Malik, *J. Hazard. Mater.*, 2004, **113**, 81–88.

3 S. S. Beheraa, S. Dasb, P. K. Parhia, S. K. Tripathyb, R. K. Mohapatrac and M. Debatac, *Desalin. Water Treat.*, 2017, **60**, 249–260.

4 (*a*) G. Crini, *Bioresour. Technol.*, 2006, **97**, 1061–1085; (*b*) V. K. Gupta and Suhas, *J. Environ. Manage.*, 2009, **90**, 2313–2342.

5 (*a*) M. Chen, M. Zhong and J. A. Johnson, *Chem. Rev.*, 2016, **116**, 10167–10211; (*b*) G. Liu, Y. M. Zhang, X. Xu, L. Zhang, Q. Yu, Q. Zhao, C. Zhao and Y. Liu, *Adv. Opt. Mater.*, 2017, **5**, 1700770; (*c*) G. Liu, J. Zhu, Y. Zhou, Z. Dong, X. Xu and P. Mao, *Org. Lett.*, 2018, **20**, 5626–5630; (*d*) G. Liu, L. Wang, Y. Zhou, N. Li, H. Zhang, J. Zhu, P. Mao and X. Xu, *Dyes Pigm.*, 2020, **172**, 107800.

6 R. A. Lorenzo, A. M. Carro and A. Concheiro, *Anal. Bioanal. Chem.*, 2015, **407**, 4927–4948.

7 (*a*) V. Ramamurthy and J. Sivaguru, *Chem. Rev.*, 2016, **116**, 9914–9993; (*b*) Y. Liu, J. Genzer and M. D. Dickey, *Prog. Polym. Sci.*, 2016, **52**, 79–106.

8 (*a*) J. Park, Q. Jiang, D. Feng and H. C. Zhou, *Angew. Chem., Int. Ed.*, 2016, **55**, 7188–7193; (*b*) J. Park, Q. Jiang, D. Feng, L. Mao and H. C. Zhou, *J. Am. Chem. Soc.*, 2016, **138**, 3518–3525; (*c*) Y. Qin, L. J. Chen, F. Dong, S. T. Jiang, G. Q. Yin, X. Li, Y. Tian and H. B. Yang, *J. Am. Chem. Soc.*, 2019, **141**, 8943–8950; (*d*) G. Liu, X. Xu, Y. Chen, X. Wu, H. Wu and Y. Liu, *Chem. Commun.*, 2016, **52**, 7966–7969; (*e*) Q. J. Hu, Y. C. Lu, C. X. Yang and X. P. Yan, *Chem. Commun.*, 2016, **52**, 5470–5473.

9 (*a*) A. M. Kloxin, A. M. Kasko, C. N. Salinas and K. S. Anseth, *Science*, 2009, **324**, 59–63; (*b*) M. U. de la Orden, J. M. Montes, J. M. Urreaga, A. Bento, M. R. Ribeir, E. Perez and M. L. Cerrada, *Polym. Degrad. Stab.*, 2015, **111**, 78–88; (*c*) L. Sun, Y. Yang, C. M. Dong and Y. Wei, *Small*, 2011, **7**, 401–406; (*d*) C. C. Chen, W. H. Ma and J. C. Zhao, *Chem. Soc. Rev.*, 2010, **39**, 4206–4219; (*e*) W. Zhao, W. H. Ma, C. C. Chen, J. C. Zhao and Z. G. Shuai, *J. Am. Chem. Soc.*, 2004, **126**, 4782–4783.

10 (*a*) S. J. Wezenberg and B. L. Feringa, *Org. Lett.*, 2017, **19**, 324–327; (*b*) M. Vlatković, B. L. Feringa and S. J. Wezenberg, *Angew. Chem., Int. Ed.*, 2016, **55**, 1001–1004; (*c*) J. Leng, G. Liu, T. Cui, S. Mao, P. Dong, W. Liu, X. Q. Hao and M. P. Song, *Dyes Pigm.*, 2021, **184**, 108838.

11 (*a*) G. Liu, Y. M. Zhang, X. Xu, L. Zhang and Y. Liu, *Adv. Opt. Mater.*, 2017, **5**, 1700770; (*b*) G. Liu, Y. M. Zhang, L. Zhang, C. Wang and Y. Liu, *ACS Appl. Mater. Interfaces*, 2018, **10**, 12135–12140.

12 (*a*) N. Kamatham, J. P. Da Silva, R. S. Givens and V. Ramamurthy, *Org. Lett.*, 2017, **19**, 3588–3591; (*b*) N. Kamatham, D. C. Mendes, J. P. Da Silva, R. S. Givens and V. Ramamurthy, *Org. Lett.*, 2016, **18**, 5480–5483; (*c*) S. E. Border, R. Z. Pavlović, L. Zhiquan and J. D. Badjić, *J. Am. Chem. Soc.*, 2017, **139**, 18496–18499; (*d*) M. A. Romero, N. Bas&lio, A. J. Moro, M. Domingues, J. A. González-Delgado, J. F. Arteaga and U. Pischel, *Chem.–Eur. J.*, 2017, **23**, 13105–13111.

13 Y. X. Wang, Y. M. Zhang and Y. Liu, *J. Am. Chem. Soc.*, 2015, **137**, 4543–4549.

14 X. Guan, Y. Chen, P. Guo, P. Li and Y. Liu, *Chem. Commun.*, 2020, **56**, 7187–7190.
15 X. Wu, Y. Chen and Y. Liu, *Adv. Sustainable Syst.*, 2019, **3**, 1800165.
16 S. Guo, X. Liu, C. Yao, C. Lu, Q. Chen, X. Y. Hu and L. Wang, *Chem. Commun.*, 2016, **52**, 10751–10754.
17 A. Loudet and K. Burgess, *Chem. Rev.*, 2007, **107**, 4891–4932.
18 (*a*) J. F. Lovell, T. W. B. Liu, J. Chen and G. Zheng, *Chem. Rev.*, 2010, **110**, 2839–2857; (*b*) M. Vendrell, D. Zhai, J. Cheng Er and Y. T. Chang, *Chem. Rev.*, 2012, **112**, 4391–4420; (*c*) T. Kowada, H. Maeda and K. Kikuchi, *Chem. Soc. Rev.*, 2015, **44**, 4953–4972.
19 (*a*) A. Kamkaew, S. H. Lim, H. B. Lee, L. V. Kiew, L. Y. Chung and K. Burgess, *Chem. Soc. Rev.*, 2013, **42**, 77–88; (*b*) Q. J. Hu, Y. C. Lu, C. X. Yang and X. P. Yan, *Chem. Commun.*, 2016, **52**, 5470–5473.
20 J. Zhao, K. Xu, W. Yang, Z. Wang and F. Zhong, *Chem. Soc. Rev.*, 2015, **44**, 8904–8939.
21 B. Yuan, H. Wu, H. Wang, B. Tang, J.-F. Xu and X. Zhang, *Angew. Chem., Int. Ed.*, 2021, **60**, 706–710.
22 (*a*) C. Li, K. Han, J. Li, Y. Zhang, W. Chen, Y. Yu and X. Jia, *Chem.–Eur. J.*, 2013, **19**, 11892–11897; (*b*) X. Wang, H. Deng, J. Li, K. Zheng, X. Jia and C. Li, *Macromol. Rapid Commun.*, 2013, **34**, 1856–1862.